Characterization of Reproductive, Metabolic, and Endocrine Features of Polycystic Ovary Syndrome in Female Hyperandrogenic Mouse Models

A. S. L. Caldwell, L. J. Middleton, M. Jimenez, R. Desai, A. C. McMahon, C. M. Allan, D. J. Handelsman, and K. A. Walters

Andrology Laboratory (A.S.L.C., L.J.M., M.J., R.D., C.M.A.,D.J.H., K.A.W.) and Biogerontology Laboratory (A.C.M.), ANZAC Research Institute, University of Sydney, Sydney, New South Wales 2139, Australia

Polycystic ovary syndrome (PCOS) affects 5–10% of women of reproductive age, causing a range of reproductive, metabolic and endocrine defects including anovulation, infertility, hyperandrogenism, obesity, hyperinsulinism, and an increased risk of type 2 diabetes and cardiovascular disease. Hyperandrogenism is the most consistent feature of PCOS, but its etiology remains unknown, and ethical and logistic constraints limit definitive experimentation in humans to determine mechanisms involved. In this study, we provide the first comprehensive characterization of reproductive, endocrine, and metabolic PCOS traits in 4 distinct murine models of hyperandrogenism, comprising prenatal dihydrotestosterone (DHT, potent nonaromatizable androgen) treatment during days 16–18 of gestation, or long-term treatment (90 days from 21 days of age) with DHT, dehydroepiandrosterone (DHEA), or letrozole (aromatase inhibitor). Prenatal DHT-treated mature mice exhibited irregular estrous cycles, oligo-ovulation, reduced preantral follicle health, hepatic steatosis, and adipocyte hypertrophy, but lacked overall changes in body-fat composition. Long-term DHT treatment induced polycystic ovaries displaying unhealthy antral follicles (degenerate oocyte and/or $>$ 10% pyknotic granulosa cells), as well as anovulation and acyclicity in mature (16-week-old) females. Long-term DHT also increased body and fat pad weights and induced adipocyte hypertrophy and hypercholesterolemia. Long-term letrozole-treated mice exhibited absent or irregular cycles, oligo-ovulation, polycystic ovaries containing hemorrhagic cysts atypical of PCOS, and displayed no metabolic features of PCOS. Long-term dehydroepiandrosterone treatment produced no PCOS features in mature mice. Our findings reveal that long-term DHT treatment replicated a breadth of ovarian, endocrine, and metabolic features of human PCOS and provides the best mouse model for experimental studies of PCOS pathogenesis. **(*Endocrinology* 155: 3146–3159, 2014)**

Polycystic ovary syndrome (PCOS) affects 5–10% of women of reproductive age (1). It is a complex, heterogeneous disorder with reproductive, endocrine, metabolic, and psychological features. Various clinical definitions are used to define PCOS, and, in general, women must have at least 2 of the following: ovulatory disturbance (or dysfunction), hyperandrogenism, and polycystic ovaries (1, 2). Apart from these hallmark features, PCOS is also characterized by reproductive hormone dysregulation involving LH hypersecretion and hyperandrogenism leading to acne and hirsutism, reduced fertility, due to dysfunctional follicular maturation, ovulatory disturbance, and miscarriage (3, 4). Nonreproductive metabolic abnormalities are also often present in women with PCOS, including obesity, metabolic syndrome, hyperinsulinemia, insulin resistance, dyslipidemia, and an increased risk of cardiovascular disease and type 2 diabetes (1, 4). Yet, despite its prevalence and health impact, the

ISSN Print 0013-7227 ISSN Online 1945-7170
Printed in U.S.A.

Received March 5, 2014. Accepted May 20, 2014.
First Published Online May 30, 2014

Abbreviations: A4, androstenedione; 3αdiol, 5α-androstane-3α,17β-diol; AR, androgen receptor; 3βdiol, 5α-androstane-3β,17β-diol; BMD, bone mineral density; BW, body weight; CV, coefficient of variation; DHEA, dehydroepiandrosterone; DHT, dihydrotestosterone; E2, estradiol; LBM, lean body mass; P4, progesterone; PCOS, polycystic ovary syndrome; T, testosterone.

etiology and pathogenesis of PCOS remain poorly understood.

Unraveling the etiology and developing novel biomarkers as well as optimal or curative treatments for PCOS remains difficult due to the heterogeneity of the syndrome and lack of understanding of its origins and pathogenic mechanisms. Due to the ethical and logistic limitations on human experimentation, suitable animal models that mimic all or most PCOS traits are indispensable. Since the 1960s a range of animal models, including rodents, sheep, and nonhuman primates, have been generated to study the pathogenesis of PCOS (3, 5–7). Prenatal exposure of sheep and nonhuman primates to androgens has provided models that show striking similarities to women with PCOS (3, 5). In utero exposure to testosterone (T) in female sheep (5, 8–10) and rhesus monkeys (3, 11, 12) induces the key PCOS-like phenotypes of oligo-ovulation or anovulation, polycystic ovaries, enhanced follicle recruitment, LH hypersecretion, and insulin resistance. However, the primate, in particular, has a long developmental period to reproductive competence, and both models are expensive, difficult to house, and are not amenable to genetic manipulations. Mouse models, on the other hand, are affordable, easy to handle and maintain, have short reproductive lifespan and generation times, and genetic manipulations are feasible. Hence, mouse models provide a valuable and versatile tool by which to allow the specific evaluation of genetic and other mechanistic pathways that may be involved in the pathogenesis of PCOS.

Numerous rodent PCOS models have been described, including treatment with androgens, estrogens, aromatase inhibitors, antiprogestins, changes in light exposure, and genetic manipulations all being used to induce PCOS-like characteristics (reviewed in Reference 6). Hyperandrogenism is the most consistent PCOS trait (3), and hence most recent studies have focused on using androgens to induce PCOS in rodent models (13–17). Rodents have been treated prenatally and postnatally with the androgens T, testosterone propionate, and DHT, and postnatally with dehydroepiandrosterone (DHEA) and letrozole, an aromatase inhibitor that blocks aromatization and the conversion of androgens to estrogens, and therefore increases circulating and ovarian androgen levels. Although postnatal treatment with T and testosterone propionate induced typical PCOS features such as acyclicity, anovulation, polycystic ovaries, hyperandrogenism, and insulin resistance (18, 19), the fact that T can be aromatized to estradiol (E2) makes it difficult to define androgen-mediated mechanisms, because steroid effects may be induced via the androgen receptor (AR) and/or the estrogen receptor. Previous studies have shown that rodents prenatally exposed to DHT exhibit irregular reproductive cycles, LH hypersecretion (16, 20), and impaired glucose tolerance but normal insulin sensitivity and body mass (17). However, polycystic ovaries are not present (16), and a comprehensive analysis of metabolic features is lacking. On the other hand, long-term treatment of rats and mice with DHT from 3 weeks of age induces acyclicity, polycystic ovaries, and key metabolic features of obesity and insulin resistance (13, 14). Results from 2 studies describing the PCOS features using a long-term DHT mouse model point toward this being an attractive model by which to assess the etiology of PCOS; however, detailed analysis of steroid profiles, cycle-matched gonadotropin levels, cholesterol and triglyceride levels, and other metabolic features are lacking. DHEA treatment of mice (21, 22) and rats (23, 24) from 3 weeks of age for 20 days parallels PCOS reproductive features of acyclicity and anovulation, but limited data are available on whether DHEA treatment induces the metabolic disturbances associated with PCOS. Lastly, no letrozole-induced mouse PCOS model has been described although rat models in which letrozole has been given for at least 21 consecutive days have been reported (14, 25, 26). Hence, there is no gold-standard rodent PCOS model, and a comprehensive comparative evaluation of all reproductive, endocrine, and metabolic characteristics taking into account potential strain differences (27) is needed. Therefore, in this study we set out to comprehensively assess reproductive, endocrine, and metabolic features associated with PCOS in 4 distinct hyperandrogenized murine models within a single mouse strain.

Materials and Methods

Mice

Mice were maintained under standard housing conditions (ad libitum access to food and water in a temperature- and humidity-controlled, 12-hour light cycle environment) at the ANZAC Research Institute. All mice had a wild-type AR genotype and were taken from a colony used to generate AR-knockout mice (28, 29). This colony has been backcrossed onto a C57Bl/6J background for at least 10 generations prior to use in experiments. In all experiments littermate controls were used. All procedures were performed under ketamine/xylazine anesthesia. All procedures were approved by the Sydney Local Health District Animal Welfare Committee within NHMRC guidelines for animal experimentation.

Generation of PCOS mouse models

Prenatal treatment

Females were paired with fertile males (a total of 6 breeding pairs) and checked daily for copulatory plugs. The date of plug was treated as day 1 of gestation. On days 16–18 of gestation, pregnant females were injected daily sc with either 100 μL sesame oil (controls) or 100 μL sesame oil containing 250 μg DHT

(Merck), as previously described (20). Female offspring (control, n = 8; and DHT, n = 12) were studied as adults at 16 weeks of age.

Postnatal treatment

At 21 days of age female mice were implanted sc with either a 1-cm SILASTIC brand implant (id, 1.47 mm; od, 1.95 mm, Dow Corning Corp, catalog no. 508–006) containing about 10 mg DHT, or one 90-day continuous-release pellet containing 7.5 mg DHEA (Innovative Research of America), or two 90-day continuous-release pellets containing 4 mg of letrozole (total 8 mg letrozole) (Letrozole provided by Novartis Pharma AG, and made into 90-day continuous-release pellet by Innovative Research of America). The experimental strategies chosen for DHT, DHEA, and letrozole were based on previous studies. DHT has previously been used to induce PCOS in rats (7.5 mg DHT 90-day continuous-release pellet (14)) and mice (2.5 mg DHT 90-day continuous-release pellet (13)). In the latter study DHT treatment of mice was reported to result in more than a 6-fold increase in serum DHT levels compared with controls (13). Using DHT-filled implants, as previously carried out in our laboratory (30), we have achieved a similar 8-fold increase in serum DHT levels, in DHT-treated mice compared with controls (Table 1). DHEA levels are consistently elevated in women with PCOS (31), and short-term postnatal treatment of mice with 6 mg/100 g body weight (BW) DHEA for 20 consecutive days induces features associated with PCOS (21, 22). To establish whether a constant long-term elevation in DHEA, as present in women with PCOS, would also induce PCOS characteristics, we implanted mice with 90-day continuous-release pellets containing 7.5 mg DHEA. Compared with controls, this resulted in more than a 3-fold increase in serum DHEA levels in DHEA-treated mice (Table 1). Previously, a rat model of PCOS used a daily letrozole dose of 400 μg (36-mg pellet) (14). Using the BW proportionality, we aimed to use a daily dose of approximately 40 μg per mouse. This was administered in a 4-mg implant for 90 days. Initial treatment of female mice with one letrozole pellet did not lead to the development of any features associated with PCOS; therefore, 2 pellets of letrozole were used in the present study. Controls received blank 1-cm SILASTIC implants. Mice were collected after 13 weeks of drug administration (control, n = 8; DHT, n = 9; DHEA, n = 7 and letrozole, n = 5), when the mice were 16 weeks of age.

Assessment of estrous cycle

Estrous cycle stage was determined daily by light microscope analysis of vaginal epithelial cell smears (32). The stage of the estrous cycle was determined based on the presence or absence of leukocytes, cornified epithelial cells, and nucleated epithelial cells. Proestrous was characterized by the presence of mostly nucleated and some cornified epithelial cells; at the estrous stage mostly cornified epithelial cells were present; at metestrus both cornified epithelial cells and leukocytes were present; and at diestrus primarily leukocytes were visible.

Specimen collection

Dissected ovaries, fat pads, heart, and liver were weighed and fixed in 4% paraformadehyde at 4°C overnight, and stored in 70% ethanol before histologic processing.

Ovary collection and follicle classification, enumeration, and health

Ovaries were fixed and then processed through graded alcohols into glycol methacrylate resin (Technovit 7100; Heraeus Kulzer). Ovaries were serially sectioned at 20 μm, stained with periodic acid-Schiff (PAS), and counterstained with hematoxylin. Total numbers of small preantral follicles (oocyte with 1.5–2 layers of cuboidal granulosa cells), large preantral follicles (oocyte surrounded by more than 2 and up to 5 layers of granulosa cells), small antral (oocyte surrounded with more than 5 layers of granulosa cells, and/or one or two small areas of follicular fluid), large antral follicles (contained a single large antral cavity), preovulatory follicles (possessed a single large antrum and an oocyte surrounded by cumulus cells at the end of a stalk of mural granulosa cells), and atretic cyst-like follicles (large fluid-filled cyst with an attenuated granulosa cell layer, dispersed theca cell layer, and an oocyte lacking connection with the granulosa cells (see Figure 3, D (iii) and H (v)). Corpora lutea and zona pellucida remnants were counted on all serial sections throughout each ovary using an Olympus microscope with Stereo Investigator software (MicroBrightField), as previously de-

Table 1. Serum Hormone and Steroid Levels in Androgenized Mouse Models

	Prenatal Treatments		Postnatal Treatments			
	Control	DHT	Control	DHT	DHEA	Letrozole
FSH (ng/mL)	5.33 ± 0.78	3.70 ± 0.73	7.16 ± 2.08	5.78 ± 0.62	5.53 ± 0.50	7.38 ± 1.48
LH (ng/mL)	2.87 ± 1.78	3.65 ± 1.47	0.30 ± 0.13	0.38 ± 0.22	5.42 ± 3.62	0.60 ± 0.36
T (ng/mL)	0.08 ± 0.03	0.03 ± 0.01	0.02 ± 0.01	0.01 ± 0.00	0.08 ± 0.02	0.29 ± 0.14[a]
A4 (ng/mL)	0.04 ± 0.01	0.04 ± 0.01	0.04 ± 0.01	0.03 ± 0.00[a]	0.08 ± 0.01[a]	0.04 ± 0.01
DHT (ng/mL)	0.18 ± 0.06	0.16 ± 0.06	0.19 ± 0.07	1.64 ± 0.32[a]	0.37 ± 0.14	0.38 ± 0.17
DHEA (ng/mL)	0.35 ± 0.09	0.18 ± 0.04	0.52 ± 0.07	0.88 ± 0.39	1.95 ± 0.39[a]	0.33 ± 0.19
3αdiol and 3βdiol (ng/mL)	0.33 ± 0.11	0.20 ± 0.04	0.30 ± 0.03	7.03 ± 0.25[a]	0.33 ± 0.04	0.20 ± 0.02
E2 (pg/mL)	7.55 ± 1.96	9.84 ± 4.65	8.45 ± 3.65	15.09 ± 8.40	6.10 ± 1.95	4.43 ± 1.18
P4 (ng/mL)	7.05 ± 3.16	1.05 ± 0.22[a]	4.55 ± 2.18	0.36 ± 0.07[a]	2.99 ± 1.58	1.71 ± 0.77

Serum levels of FSH, LH, T (long-term letrozole treatment, $P < .01$), A4 (long-term DHT and DHEA treatment, $P < .01$), DHT (long-term DHT treatment, $P < .01$), 3α- and 3β-diol (long-term DHT treatment, $P < .01$), E2, and P4 (prenatal DHT treatment, $P \leq .01$, and long-term DHT treatment, $P < .01$). Data are the mean ± SEM (n = 5–9 per treatment group).

[a] Denotes a statistically significant difference.

scribed (28, 32, 33). For all analyses, large antral follicles and preovulatory follicles were grouped together and called large antral follicles. For all histologic analyses, repetitive counting of follicles was avoided by only counting/measuring follicles containing an oocyte with a visible nucleolus. To avoid bias, all ovaries were analyzed without knowledge of treatment group. Follicles were classified as unhealthy if they contained a degenerate oocyte and/or more than 10% of the granulosa cells were pyknotic in appearance, as previously described (28). The proportion of unhealthy follicles per ovary was estimated as the percentage of all follicles at that developmental stage. For all large antral follicles, granulosa cell layer thickness and theca layer area were measured using ImageJ v1.44 software (open source, developed by National Institutes of Health).

Hormone assays

Blood was collected from females at the diestrous stage (unless females were acyclic) by cardiac exsanguination under ketamine/xylazine anesthesia, and collected serum was stored at −20°C. Mouse serum LH and FSH were determined using a species-specific immunofluorometric assay, as previously described (32, 34, 35). The mLH detection limit was 0.04 ng/mL, the intraassay coefficient of variation (CV) was 5.2%, and the interassay CV was 8.6%. The mFSH detection limit was 0.1 ng/mL, the intraassay CV was 3.1%, and the interassay CV was 7.2%. All immunoassays were performed in a single batch.

Serum levels of testosterone (T), androstenedione (A4), DHEA, DHT, and its 2 principal metabolites 5α-androstane-3α,17β-diol (3αdiol) and 5α-androstane-3β,17β-diol (3βdiol), E2, and progesterone (P4) were measured in extracts of 100 μL mouse serum by liquid chromatography-tandem mass spectrometry (36) as adapted for mouse serum (37) and further modified (Supplemental *Materials and Methods*). The limits of quantitation (defined as lowest level that can be detected with a CV of < 20%) were T (25 pg/mL), A4 (25 pg/mL), DHEA (100 pg/mL), DHT (100 pg/mL), 3αdiol (100 pg/mL), 3βdiol (100 pg/mL), E2 (2.5 pg/mL), and P4 (50 pg/mL). To characterize DHT metabolism, the sum of DHT's two major primary metabolites 3αdiol and 3βdiol was calculated.

Body mass analysis–PIXImus

Body composition measurements were performed on a Lunar PIXImus Densitometer for mice (GE Medical Systems), as previously described (38).

Adipose tissue histology

Parametrial and retroperitoneal fat pads were fixed in 4% paraformaldehyde, embedded in paraffin, sectioned at 8 μm, stained with hematoxylin and eosin, and evaluated by histomorphometry at ×40 magnification, using an Olympus microscope with Stereo Investigator software (MicroBrightField).

Hepatic steatosis analysis

Liver sections were embedded in paraffin, sectioned at 5 μm, and stained with hematoxylin and eosin before histomorphometric analysis. The presence of steatosis was microscopically quantified blindly by 2 independent investigators by classification into 4 different categories (0 = nonfatty liver; 1 = possible early steatosis; 2 = moderate steatosis; 3 = severe steatosis; as outlined in a previous study (39)). There were no disagreements in the classifications between the 2 investigators.

Triglyceride and cholesterol assays

Serum levels of total cholesterol and triglycerides were assayed enzymatically with commercial kits obtained from Wako (Cholesterol E kit, catalog no. 439–17501; and Triglyceride E kit, catalog no. 342–40201).

Insulin tolerance tests

Insulin tolerance tests were carried out, as previously described (38). Mice were fasted for 6 hours prior to baseline blood glucose reading, followed by an ip injection of insulin at 0.75 IU/kg BW (Eli Lilly). Blood glucose was then measured at 15, 30, 60, 90, and 120 minutes after insulin injection. Blood was obtained from a tail prick, and blood glucose was measured on glucose strips and an Accu-Chek glucometer (Roche). Measurements were taken at the start and end of each experiment. Blood glucose data are presented as percentage of baseline blood glucose.

Statistical analysis

Statistical analysis was performed using NCSS 2007 software (NCSS Statistical Software). Data that were not normally distributed were transformed prior to analysis using a log transformation. Statistical differences were tested by *t* test or ANOVA with post hoc test using Fisher's LSD Multiple-Comparison Test. Proportions were analyzed by Fisher's exact test or Kruskal-Wallis exact test. All parametric tests were confirmed by the analogous nonparametric tests. P values $< .05$ were considered statistically significant.

Results

Cyclicity

Prenatal treatments

All females treated prenatally with oil (control) cycled (8 of 8), whereas 50% of females treated prenatally with DHT (6 of 12) failed to cycle ($P < .05$) (Figure 1, A and C) and completed significantly fewer estrous cycles in 2 weeks (0.5 ± 0.2 vs 2.5 ± 0.2; $P < .01$) (Figure 1B).

Postnatal treatments

All DHT-treated (9 of 9, 100%) and most letrozole-treated (3 of 5, 60%) females failed to cycle ($P < .05$), whereas all DHEA-treated (7 of 7, 100%) and control (8 of 8, 100%) mice cycled regularly (Figure 1, D and F). Similarly, the number of estrous cycles completed in 2 weeks was zero for DHT and reduced for letrozole females (0.8 ± 0.6) compared with DHEA (2.4 ± 0.3) and control (2.1 ± 0.3) females (Figure 1E, $P < .01$). The letrozole-treated females that did cycle exhibited irregular cycles (Figure 1F). Observation of vaginal smears identified leukocytes as the predominant cell type observed in the vag-

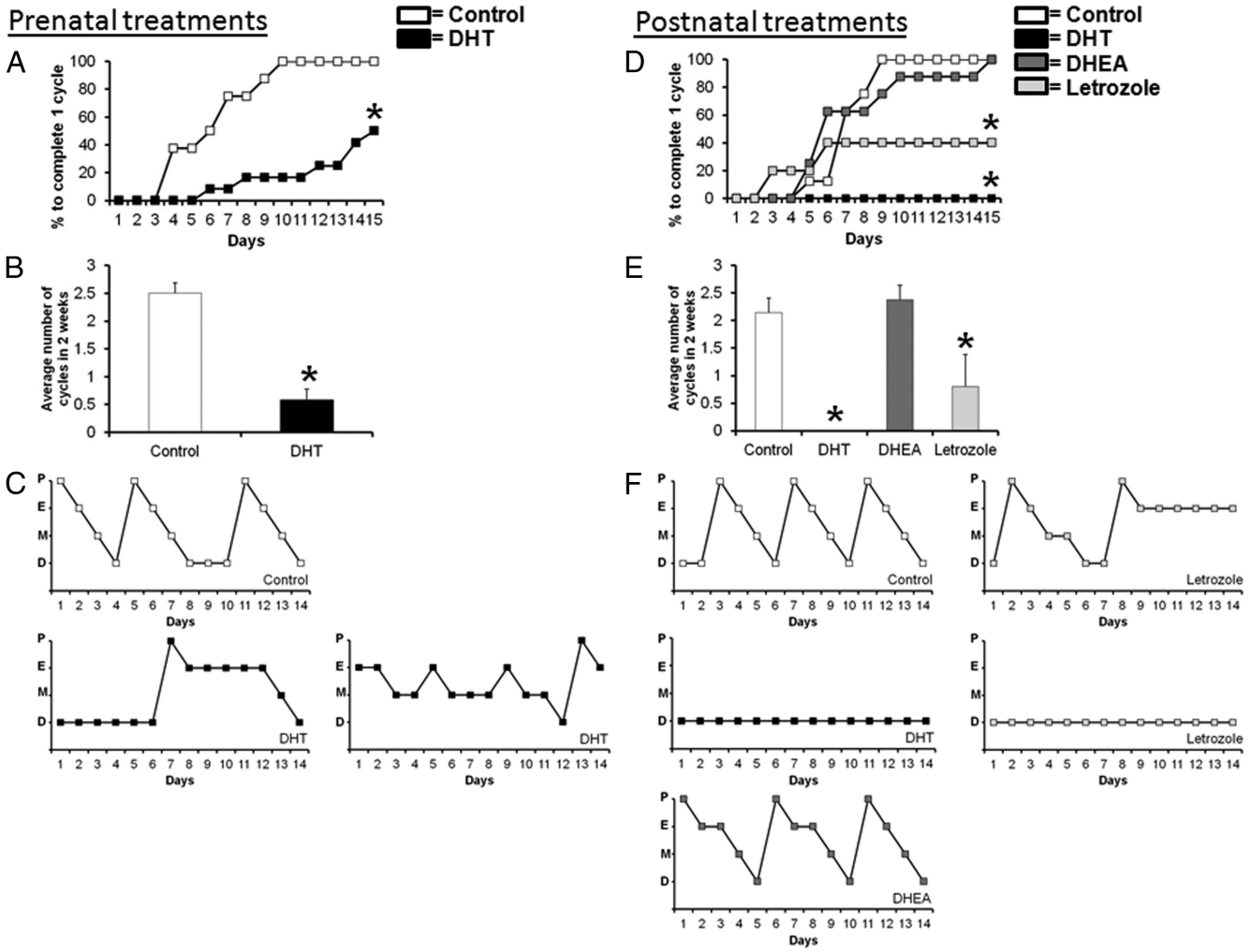

Figure 1. Estrous cycling**.** A and D, Percentage of females to complete one cycle in 2-week period. A ($P < .05$) and D ($P < .01$). B and E, Average number of cycles in 2-week period. A ($P < .01$) and D ($P < .01$). Data are the mean ± SEM (n = 5–12/treatment group). C and F, Estrous cycle pattern in representative females. P, proestrus; E, estrus; M, metestrus; D, diestrus.

inal smears from DHT- and letrozole-treated females, indicating that they were static in pseudodiestrus.

Ovary weight and ovarian follicle populations

Prenatal treatments

Ovary weight (4.6 ± 0.1 vs 5.8 ± 0.4; $P < .01$) and corpora lutea numbers (5.0 ± 0.4 vs 9.75 ± 1.79; $P < .05$) were both significantly reduced in prenatal DHT-treated females compared with controls (Figure 2, A and B). Prenatal DHT ovaries featured more follicles with an atretic cyst-like appearance (5.5 ± 1.2 vs 0.0 ± 0.0; $P < .01$) but otherwise did not exhibit the classic polycystic appearance (Figure 2, C and D). Growing follicle populations did not differ between prenatal DHT and oil (control) groups (Figure 2D).

Postnatal treatments

Ovary weight did not differ between DHT (4.1 ± 0.2)-, DHEA (4.5 ± 0.4)-, or letrozole (6.6 ± 1.0)-treated and control females (5.0 ± 0.6) (Figure 2E). Corpora lutea numbers were reduced in DHT (0 ± 0)- and letrozole (2.6 ± 1.6)-treated females compared with DHEA (9.0 ± 1.8) and control females (10.8 ± 2.1) ($P < .01$) (Figure 2F). DHT-treated females exhibited multicystic ovaries, whereas letrozole treated ovaries displayed hemorrhagic cysts, atypical of PCOS (Figure 2G). Compared with controls, the number of follicles with an atretic cyst-like appearance was significantly increased in ovaries from DHT mice (12.4 ± 3.1 vs 4.8 ± 2.2; $P < .05$). There was no significant difference in growing follicle populations in DHT-, DHEA-, and letrozole-treated mice compared with control ovaries (Figure 2H).

Ovarian follicle health and morphology

Prenatal treatments

Ovaries from prenatally DHT-treated females exhibited a significant increase in the percentage of morpho-

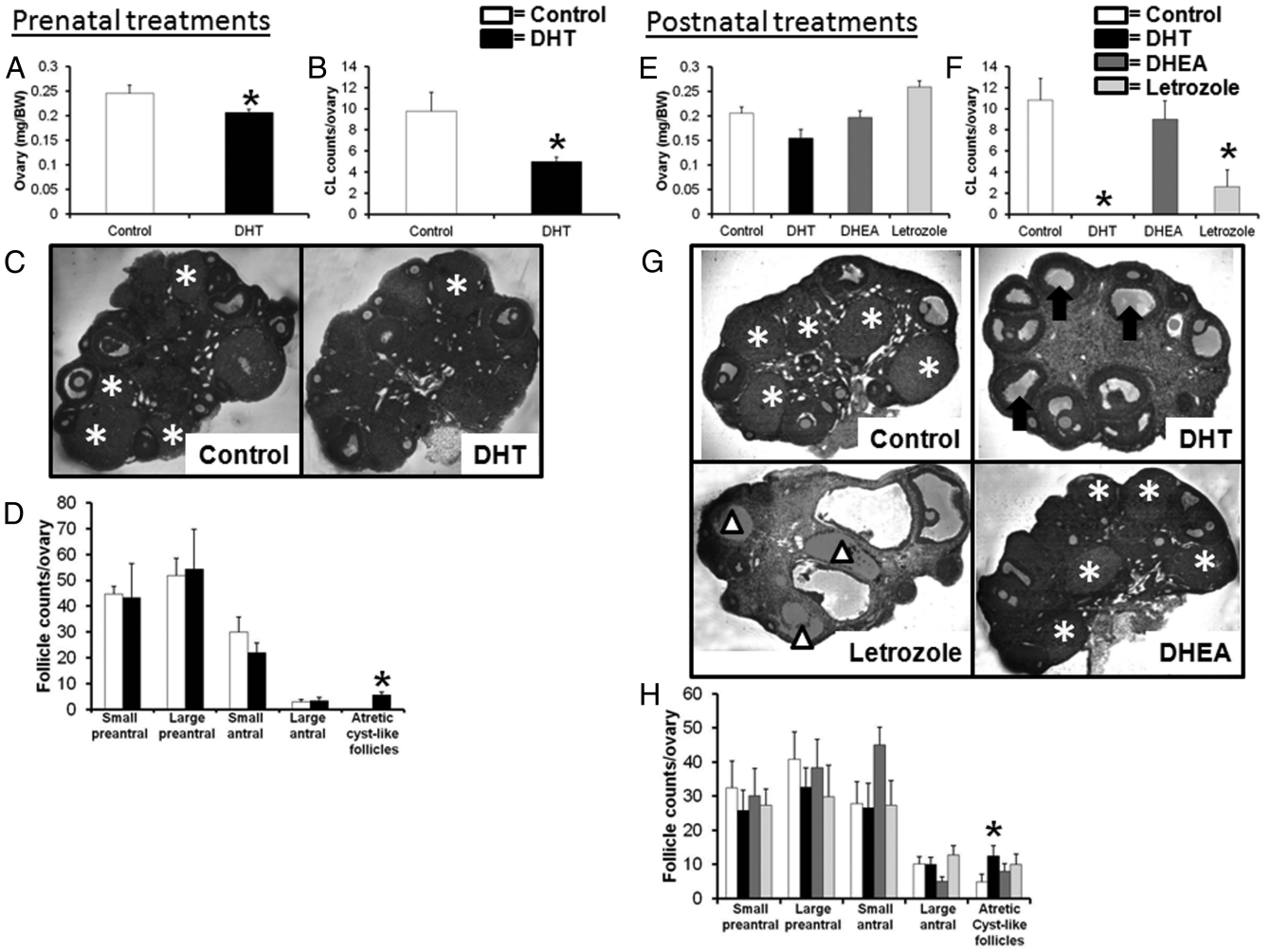

Figure 2. Ovary weight, ovarian phenotype, and ovarian follicle and corpora lutea numbers**.** A and E, Ovary weights. A ($P < .01$). Data are the mean ± SEM (n = 5–12/treatment group). B and F, Average number of corpora lutea/ovary. B ($P < .05$) and F ($P < .01$). Data are the mean ± SEM (n ≥ 4/treatment group). C and G, Histologic sections of representative ovaries from each treatment group. White asterisk, corpora lutea; black arrow, arrested large antral follicle; white triangle, hemorrhagic cyst. D and H, Average number of growing follicles/ovary. D ($P < .01$) and H ($P < .05$). Data are the mean ± SEM (n ≥ 4/treatment group).

logically unhealthy small and large preantral follicles present, compared with control ovaries (small preantral, 20.3 ± 3.9% vs 1.6 ± 1.0%; and large preantral, 20.2 ± 3.2% vs 6.0 ± 1.3%) ($P < .01$) (Figure 3A). The number of zona pellucida remnants within ovaries did not differ between treatment groups (data not shown). In large antral follicles, there was no significant difference in granulosa cell layer thickness or theca cell layer area between prenatal DHT and control females (Figure 3, B, C, and D(i) and (ii)).

Postnatal treatments

DHT (60.4 ± 11.6%)- and letrozole (45.9 ± 5.5%)-treated mice exhibited a significant increase in the percentage of morphologically unhealthy large antral follicles present within their ovaries, compared with DHEA (23.2 ± 6.7%) or control (20.6 ± 6.2%) females ($P < .01$) (Figure 3E). The number of zona pellucida remnants within ovaries did not differ between any treatment group (data not shown). Atretic follicles in control mice exhibited a compact theca cell layer; however the theca layer of atretic follicles in DHT and letrozole mice appeared to be dispersing, and there was not a discrete separation between the theca cell layer and the surrounding stroma. Large antral follicles within both DHT (59.4 ± 3.1 μm)- and letrozole (45.9 ± 5.5 μm)-treated ovaries exhibited a significant decrease in the thickness of the granulosa cell layer compared with DHEA (77.8 ± 2.1 μm) or controls (72.8 ± 2.2 μm) ($P < .01$) (Figure 3, F and H (i-iv)). The theca cell layer area of large antral follicles was significantly increased in DHT-treated ovaries (23.2 ± 0.5% theca area per follicle) but decreased in letrozole-treated ovaries (17.4 ± 0.5% theca area per follicle), compared with DHEA (19.9 ± 0.7% theca area per follicle) or control ovaries (19.1 ± 0.3% theca area per follicle) ($P < .01$) (Figure 3, G and F (i-iv)).

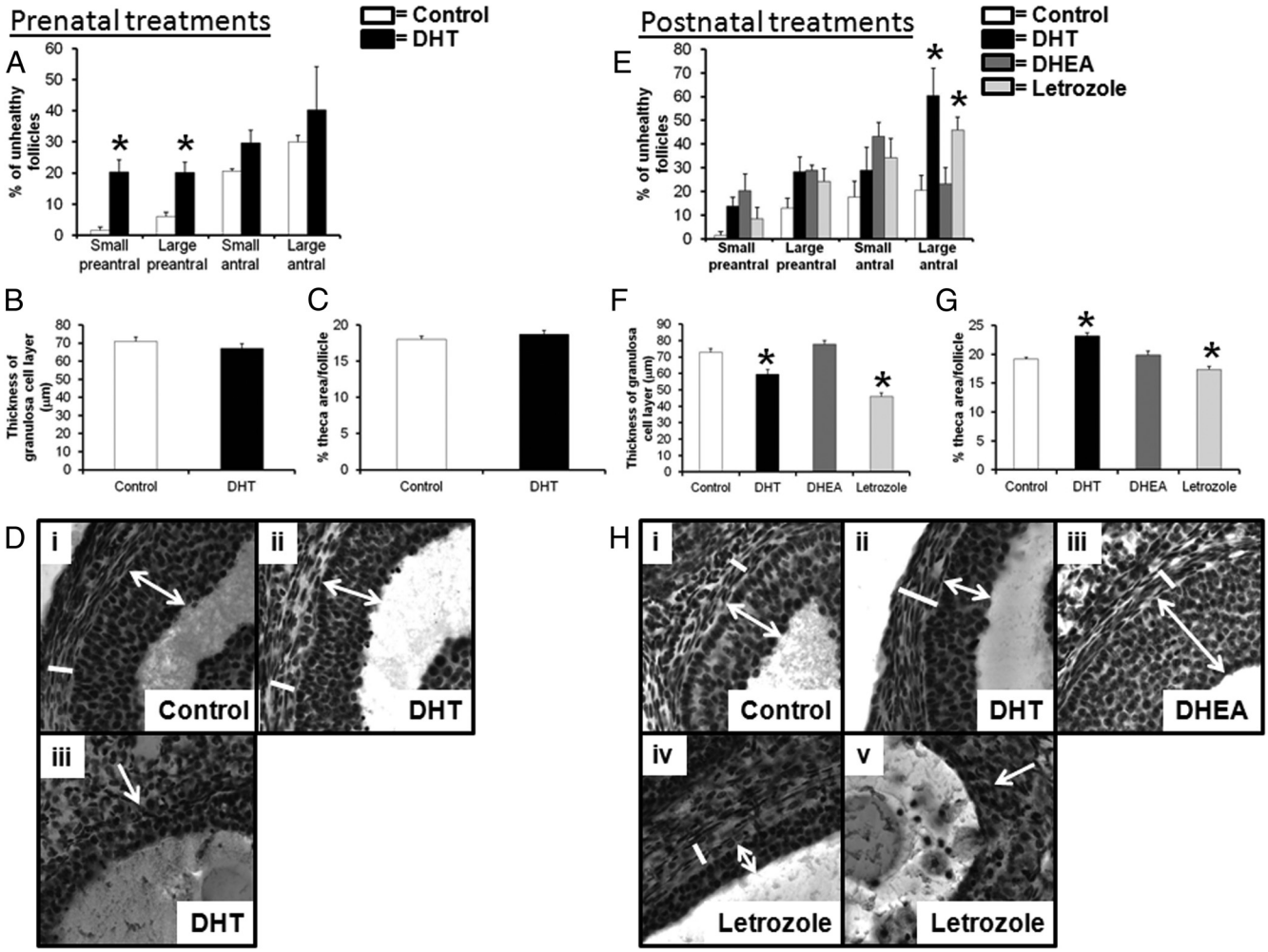

Figure 3. Ovary follicle health and morphology. A and E, Percentage of unhealthy follicles. A ($P < .01$) and E ($P < .01$). Data are the mean ± SEM (n ≥ 4/treatment group). B and F, Average thickness of granulosa cell layer. F ($P < .01$). Data are the mean ± SEM (n ≥ 15–36 follicles/treatment group). C and G, Average percentage theca cell area per follicle. G ($P < .01$). Data are the mean ± SEM. (n ≥ 15–36 follicles per treatment group). D(i and ii) and H(i-iv), Histologic sections of representative follicles from each treatment group. Double-arrowed white line, granulosa cell layer thickness; white line, theca cell layer thickness. D(iii) and H(v), Histologic sections of representative cysts from each treatment group showing attenuated granulosa cell layer, dispersed theca cell layer (white arrow), and an oocyte lacking connection with the granulosa cells.

Serum FSH and LH concentrations

Prenatal treatments

Serum levels of FSH and LH were not significantly different between control and DHT prenatally treated groups at diestrus (Table 1).

Postnatal treatments

Serum levels of FSH and LH were not significantly different between any of the treatment groups at diestrus (Table 1).

Serum steroid levels

Prenatal treatments

At diestrus, serum P4 levels were decreased by 85% in DHT females compared with controls ($P \leq .05$) (Table 1). Serum levels of T, A4, DHT, DHEA, 3αdiol, 3βdiol, and E2 did not differ between females treated prenatally with DHT or controls (Table 1).

Postnatal treatments

At diestrus, only letrozole-treated mice exhibited a significant increase in T levels compared with control females (0.29 ± 0.14 ng/mL vs 0.02 ± 0.01 ng/mL) ($P < .01$) (Table 1). Serum A4 levels were decreased by 33% in DHT females, increased by 100% in DHEA females, but not altered in letrozole females compared with control females ($P < .01$) (Table 1). As expected, there was more than 8-fold increased serum DHT levels in DHT females compared with control females ($P < .01$), but DHT levels were not altered in any other long-term treatment group (Table 1). There was more than 3-fold increase in serum DHEA levels in DHEA females, but no change in DHT and letro-

zole mice, compared with control females ($P < .01$) (Table 1). Serum levels of 3αdiol and 3βdiol (two primary DHT metabolites) were only significantly increased in DHT females compared with control females (7.03 ± 0.25 ng/mL vs 0.3 ± 0.03 ng/mL) ($P < .01$) (Table 1). There was no significant difference in E2 levels between any of the treatment groups. DHT females were the only long-term group to exhibit a significant decrease in serum P4 compared with control females (0.36 ± 0.07 ng/mL vs 4.55 ± 2.18 ng/mL) ($P < .01$) (Table 1).

BW and body composition

Prenatal treatments

Dual-energy x-ray absorptiometry analysis of BW, fat, lean body mass (LBM), and bone mineral density (BMD) did not differ between prenatal DHT or control females (Figure 4A).

Postnatal treatments

Compared with control females, DHT females exhibited a 9% increase in BW ($P < .01$), a 16% increase in body fat ($P < .01$), a 7% increase in LBM ($P < .01$), but a 6% decrease in BMD ($P < .01$) (Figure 4B). DHEA females exhibited a 9% decrease in BW ($P < .01$), a 7% decrease in LBM ($P < .01$), but a 4% increase in BMD ($P < .01$) (Figure 4B). There was no difference in BW, body fat, LBM, or BMD between letrozole and control groups (Figure 4B).

Adipose tissue weight and histology

Prenatal treatments

Fat depot weights did not differ between control and prenatal DHT females (Figure 5A). However, there was a 57% increase in adipocyte size in parametrial ($P < .05$) but not retroperitoneal fat depots (Figure 5B).

Postnatal treatments

DHT treatment resulted in a 49% increase in inguinal and a 134% increased in retroperitoneal fat depot weights compared with controls ($P < .01$) (Figure 5C). Adipocyte cell size was increased by 70% in retroperitoneal ($P < .01$), but not parametrial, fat depots from DHT females (Figure 5D). There was no significant difference in fat depot weights or adipocyte cell size between DHEA or letrozole and control females (Figure 5, C and D).

Serum cholesterol and triglyceride concentrations

Prenatal treatments

There was no significant difference in serum total cholesterol and triglyceride levels between prenatal control and DHT females (Figure 6, A and B).

Postnatal treatments

Serum total cholesterol was increased by 47% in DHT-treated females compared with controls ($P < .05$) (Figure 6F). There was no significant difference in serum total cholesterol between control, DHEA, and letrozole groups,

Prenatal treatments

A	Control	DHT
BW (g)	23.1 ± 0.9	21.8 ± 0.4
Body fat (g)	5.2 ± 0.6	4.7 ± 0.5
LBM (g)	18.2 ± 0.5	17.2 ± 0.3
BMD (g/cm^2)	0.052 ± 0.001	0.052 ± 0.001

Postnatal treatments

B	Control	DHT	DHEA	Letrozole
BW (g)	23.2 ± 0.4	25.2 ± 0.6 *	21.1 ± 0.8 *	24.5 ± 0.8
Body fat (g)	4.4 ± 0.1	5.1 ± 0.3 *	3.7 ± 0.3	4.5 ± 0.3
LBM (g)	18.7 ± 0.3	20.1 ± 0.3 *	17.4 ± 0.6 *	20.0 ± 0.6
BMD (g/cm^2)	0.053 ± 0.001	0.050 ± 0.001 *	0.055 ± 0.001 *	0.051 ± 0.001

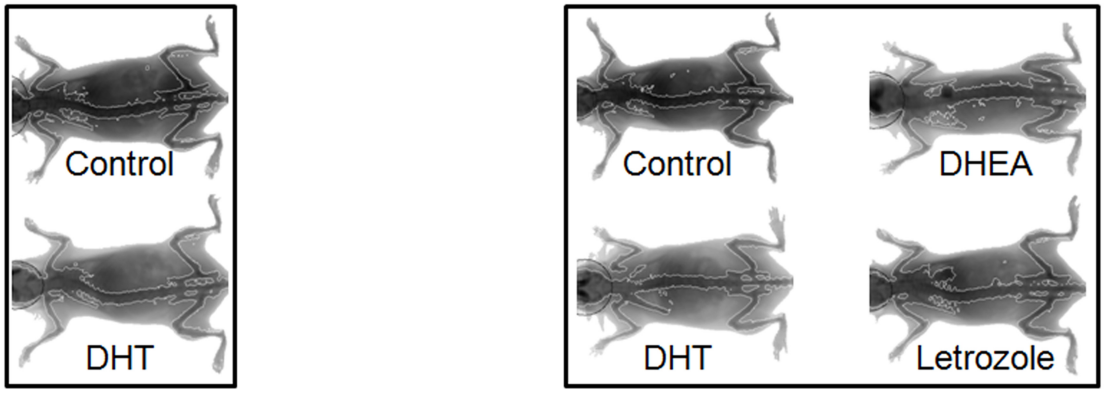

Figure 4. BW and composition**.** A and B, BW and composition calculated by dual-energy x-ray absorptiometry and representative dual-energy x-ray absorptiometry images from each treatment group (n = 5–12/treatment group).

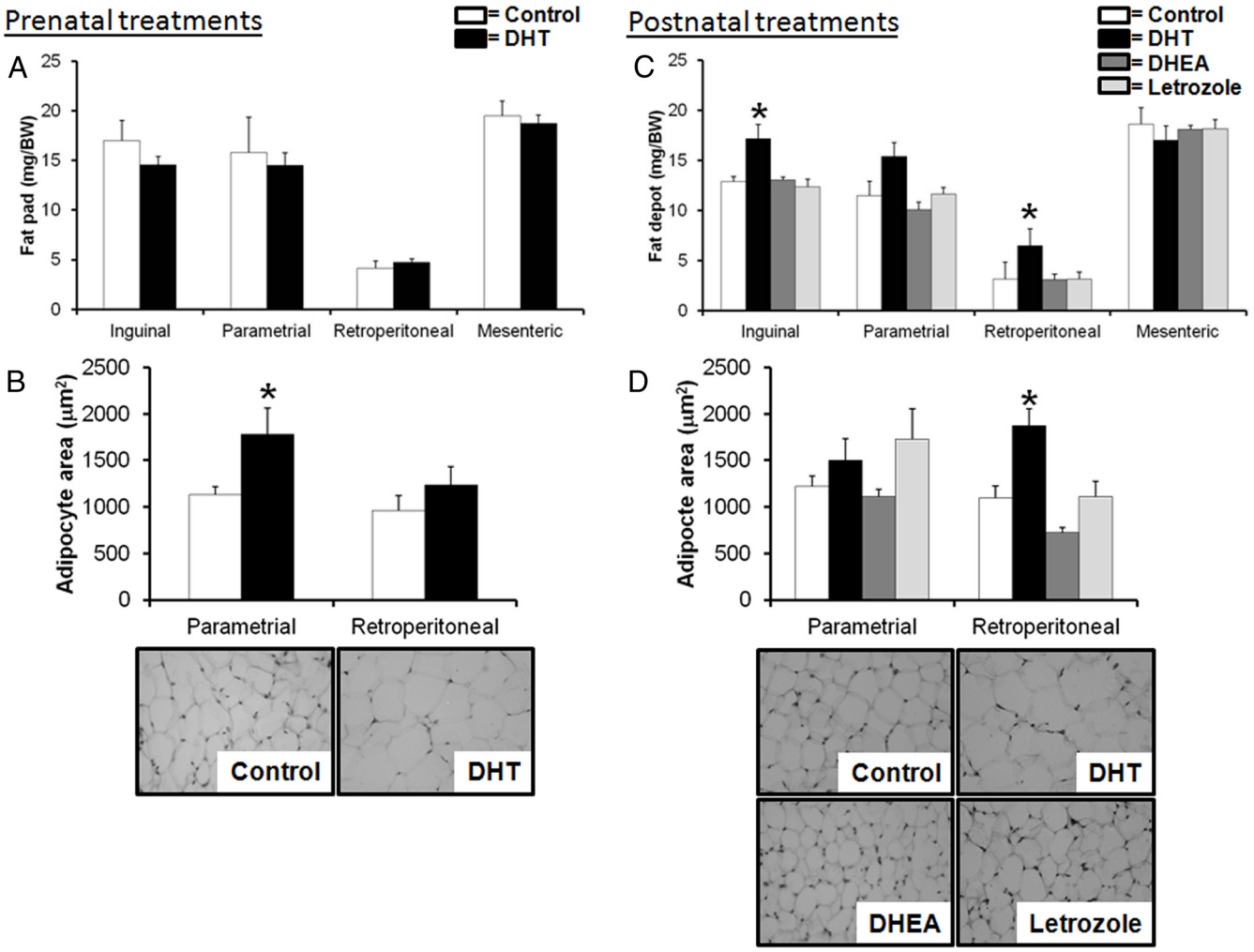

Figure 5. Fat depot weight and adipocyte size**.** A and C, Fat depot weights. C ($P < .01$). Data are the mean ± SEM. B and D, Adipocyte size. B ($P < .05$) and D ($P < .01$). Data are the mean ± SEM (n = 4–5/treatment group). Histologic sections of representative fat pads from each treatment group.

or serum triglyceride levels between any of the treatment groups (Figure 6, F and G).

Insulin tolerance

Prenatal treatments

At 16 weeks of age, fasting glucose levels (control, 8.2 ± 0.5 mmol/L; DHT, 7.8 ± 0.3 mmol/L) or insulin sensitivity (as indicated by serial blood glucose in the insulin tolerance test) were not different between control and prenatal DHT mice (Figure 6, C and D).

Postnatal treatments

At 16 weeks of age, fasting glucose levels were not different between any of the treatment groups (control, 7.3 ± 0.2 mmol/L; DHT, 8.1 ± 0.3 mmol/L; DHEA, 7.8 ± 0.4 mmol/L; letrozole, 6.8 ± 0.5 mmol/L). There was no difference in insulin sensitivity prior to (3 weeks of age) and after (16 weeks of age) treatment with DHT, DHEA, or letrozole compared with controls (Figure 6, H and I).

Heart tissue weight

Prenatal treatments

Prenatal DHT treatment resulted in a significant decrease in heart weight compared with control females prenatally treated with oil (control, 5.9 ± 0.2 mg/BW; DHT, 5.4 ± 0.1 mg; $P < .05$).

Postnatal treatments

There was no significant difference in heart weights between any of the treatment groups (control, 5.9 ± 0.3 mg/BW; DHT, 6.2 ± 0.2 mg/BW; DHEA, 6.0 ± 0.2 mg/BW; letrozole, 6.8 ± 0.1 mg).

Liver tissue weight and histology

Prenatal treatments

Prenatal DHT treatment did not alter liver weight compared with control females (control, 51.5 ± 1.5 mg/BW; DHT, 48.1 ± 1.4 mg/BW). However, prenatal treatment

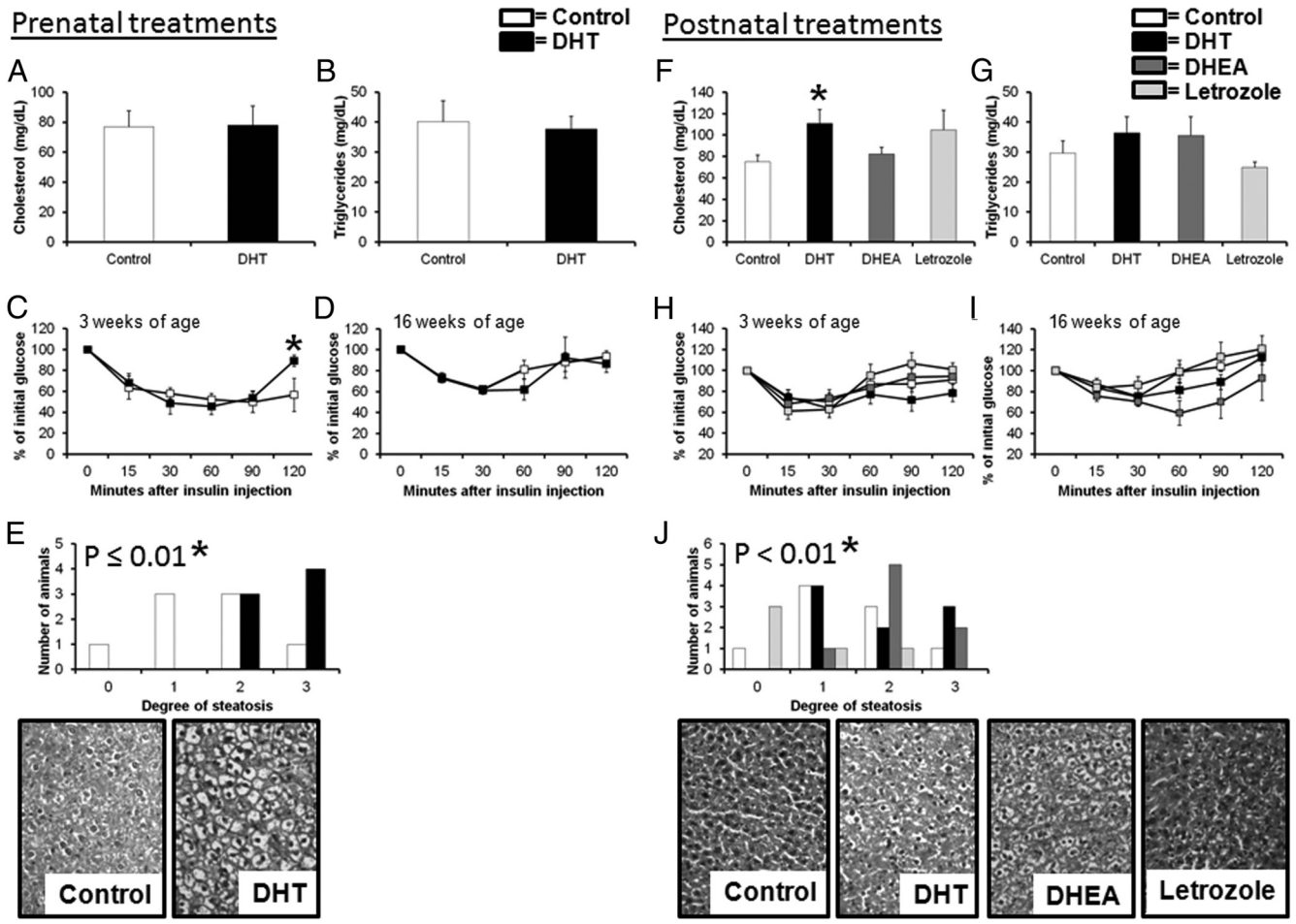

Figure 6. Serum cholesterol and triglyceride levels, insulin tolerance tests and steatosis analysis. A and F, Serum cholesterol levels. F ($P < .01$). Data are the mean ± SEM (n = 5–6/treatment group). B and G, Serum triglyceride levels. Data are the mean ± SEM (n = 5–6/treatment group). C and H, Insulin tolerance test at 3 weeks of age. D and I, Insulin tolerance test at 16 weeks of age. Data are the mean ± SEM. E and J, Degree of steatosis. E ($P \leq .01$) and J ($P < .01$) (n = 5–9/treatment group). Histologic sections of representative livers from each treatment group.

with DHT resulted in a significant increase in the presence of fatty livers (hepatic steatosis) ($P \leq .01$) (Figure 6E).

Postnatal treatments

There was no significant difference in liver weights between control females and females postnatally treated with DHT, DHEA, or letrozole (control, 44.5 ± 2.8 mg/BW; DHT, 50.6 ± 2.1 mg/BW; DHEA, 47.6 ± 2.2 mg/BW; letrozole, 42.8 ± 3.0 mg/BW). The extent of hepatic steatosis was different between treatment groups, with DHT and DHEA treatment producing more severe steatosis than control and letrozole mice ($P < .01$) (Figure 6J).

Discussion

This study provides the first comprehensive characterization and evaluation of reproductive, endocrine, and metabolic PCOS traits in 4 distinct hyperandrogenized female murine models of PCOS. We have established the first letrozole and long-term DHEA mouse models and compared them with prenatal DHT and long-term DHT androgenized murine models. Our finding show that only the in vivo elevation of the potent bioactive androgen DHT, but not the proandrogen DHEA, induces features that in mice replicate PCOS traits, including irregular estrous cycling with oligoanovulation, polycystic ovaries, obesity, dyslipidemia, and hepatic steatosis. Genetic and environmental factors contribute to the development of PCOS (40). Importantly, in this study differences in strain-specific responses, such as those previously observed for metabolic response to excess androgen exposure during puberty (41), were controlled for by all experimental mice arising from a single mouse strain. Our findings have identified the superiority of long-term DHT treatment in mice, as overall the best approach to simulate the breadth of reproductive, endocrine, and metabolic features of human PCOS (Table 2 summarizes features of the androgenized mouse models relative to PCOS).

Table 2. Summary of Dysfunctional Reproductive, Endocrine and Metabolic Traits in PCOS Women and the Androgenized Mouse Models Examined in the Current Study

Human Diagnostic Traits of PCOS	Prenatal Treatment	Postnatal Treatments		
	DHT	DHT	DHEA	Letrozole
Irregular cycles/acyclicity	✓	✓	X	✓
Oligo- or anovulation	✓	✓	X	✓
Hyperandrogenism (↑ in T)	X	X	X	✓
LH hypersecretion	X	X	X	X
↓ Progesterone	✓	✓	X	X
Multicystic ovaries	X	✓	X	✓[a]
↑ Ovary weight	X	X	X	X
↑ Preantral follicles	X	X	X	X
Antral follicle arrest	X	✓	X	✓
↑ Follicle atresia	✓	✓	X	✓
↓ Granulosa cell layer thickness	X	✓	X	✓
↑ Theca cell layer thickness	X	✓	X	X
↑ Obesity	X	✓	X	X
Adipocyte hypertrophy	✓	✓	X	X
Dyslipidemia	X	✓	X	X
Insulin resistance	X	X	X	X
Presence of steatosis	✓	✓	✓	X

✓, present; X, not present.

[a] Hemorrhagic cysts which are not a true PCOS phenotype

In our study prenatal DHT, and long-term DHT, or letrozole treatment induced irregular cycles or acyclicity, but long-term DHEA treatment had no effect on estrous cyclicity. In concordance, vaginal smears revealed that long-term DHT treatment left females fixed in pseudodiestrus, whereas prenatal DHT or letrozole treatment produced females that spent little time in proestrus, the prelude to ovulation. Our findings support previous observations of disrupted estrous cycles in rodents treated prenatally (16, 20) or postnatally (13, 14) with DHT, and rats treated with letrozole (14, 25) but differ from findings in mice treated with DHEA (21, 24). Acyclicity in long-term DHT females, indicative of anovulation, was confirmed by lack of corpora lutea and reduced serum P4 levels. Acyclicity without elevated gonadotropin levels in all long-term DHT females implies aberrant neuroendocrine regulation of ovarian function, although this cannot exclude additional and contributory defects at the ovary level. Reduced corpora lutea numbers in some female mice treated prenatally with DHT, and with letrozole, is consistent with ovulatory dysfunction and the wide heterogeneity of ovarian cycling patterns in PCOS (2). By contrast, long-term DHEA-treated females maintained regular estrous cycling, did not differ from controls in circulating T or P4 concentrations, and displayed continued regular ovulation, evident by fresh corpora lutea. These findings differ from previous studies of rodents treated with DHEA for 20 days in which elevated circulating T concentrations and irregular estrous cycles or acyclicity were observed (21, 22, 24). In concert, these findings suggest that whereas short-term DHEA treatment may disrupt central neuroendocrine regulatory mechanisms, this disruption is transient and not sustained over 3 months in this longer term study.

We found that prenatal DHT treatment induced some ovarian morphologic features of PCOS, including fewer corpora lutea and an increased prevalence of atretic cyst-like follicles, although not the classic polycystic appearance. Reduced ovarian weights of prenatal DHT-treated mice may reflect fewer corpora lutea and/or absence of PCOS-like morphologic features such as numerous large fluid-filled cysts or theca cell hyperplasia that enlarge the ovary. We used the pure androgen DHT in our prenatal androgenized group, but this does not exclude that estrogen receptor mechanisms may also be involved. In utero excess of androgens or estrogens results in anovulation and hyperandrogenism (42); however, our animal models and others (rodent, sheep, and primate) confirm that prenatal androgen excess more closely mimics the ovarian phenotype of human PCOS (6, 42). Long-term DHT treatment induced a wide spectrum of ovarian PCOS traits, including a classic multicystic ovary exhibiting large arrested and atretic cyst-like follicles, more unhealthy large antral follicles displaying thick theca cell layers, and thin degenerate granulosa cell layers, in agreement with previous findings in related DHT-induced rodent models of PCOS (13, 14). Surprisingly, androgenized mouse models in the present study did not exhibit the PCOS characteristic of increased ovarian preantral and antral follicles numbers (43). This was unexpected because androgens stimulate follicle development (44–46) and previous prenatally androgen-induced rodent (16), sheep (47, 48), and primate (49) models have reported increased preantral and antral follicle populations. These findings may imply that elevated androgen exposure may be required during specific time windows for aberrant follicle development to occur, consistent with previous findings in a rat model (15). In our work, letrozole treatment resulted in the expected increase in circulating T concentrations, reflecting the block in aromatase activity and accumulation of endogenous ovarian androgen secretion. Furthermore, ovaries from letrozole-treated females exhibited some reproductive features of PCOS, including a greater frequency of atretic cystic-like follicles, more unhealthy large antral follicles, and the majority, but not all ovaries, resembled human polycystic ovaries with the appearance of large cysts with an attenuated granulosa cell layer. However, these

were hemorrhagic cystic follicles, which are atypical of PCOS ovaries and more in keeping with several genetic mouse lines with defective ovarian function such as the aromatase knockout (50), estrogen receptor-α knockout (51), and the transgenic FSH-overexpressing (52) mice. These latter models have in common elevated gonadotropins, especially LH, with corresponding high circulating T concentrations. By contrast, in the present study, serum LH at diestrus remained normal in the letrozole-treated mice, although we cannot exclude increased pulsatile LH secretion at other stages of the estrous cycle stimulating the cystic growth of follicles. In concert, these findings suggest that elevated LH per se may not be a key factor causing classical PCOS development. Unexpectedly, sustained DHEA delivery had no long-term effects on ovarian morphology or follicle function in our 3-month study, contrasting with the reported induction of polycystic ovaries and anovulation due to short-term (20 day) DHEA administration (22, 24, 53). Hence, we proposed that the reported effects of short-term DHEA treatment may be transient rather than permanent features and may reflect that the elevated DHEA levels present in PCOS patients (54) are unlikely to cause/maintain the ovarian features of human PCOS.

Long-term exposure to DHT induced several features that are consistent with metabolic features of PCOS. Postnatally DHT-treated females exhibited increased BW and adiposity, and adipocyte hypertrophy was present in retroperitoneal fat pads, which is known to alter levels of adipokines (55) and has been implicated in the pathophysiology of PCOS (56, 57). In addition, DHT-treated females exhibited hypercholesterolemia, which is present in women with PCOS, and is a risk factor for cardiovascular disease (58). Prenatal DHT treatment did not alter BW, body fat, and lean body mass, which is in agreement with earlier findings showing that prenatally androgenized rodents do not exibit altered body composition (15, 17). Adipocyte hypertrophy was present in parametrial fat pads, but total fat depot weights were not changed. This observation supports previous work showing that androgen exposure in a mouse model alters adipocyte differentiation and/or function (17). Whether or not changes in adipocyte function play a role in the etiology of PCOS remains to be determined. Despite the presence of hypertrophic adipocytes, which are inherently insulin resistant (59), in prenatal and long-term DHT females, insulin resistance was not detected in any of the 4 androgenized mouse models. This may reflect the fact that muscle and/or liver, but not adipose tissue, are the main determinants of overall body insulin sensitivity. However, the possibility that the mice in our experiments were still too young to fully display age-related insulin resistance cannot be ruled out. Whereas most previous publications using PCOS-induced rodent models did not address insulin sensitivity, in 3 studies postnatal DHT (14), DHEA (21), and letrozole (26) treatment was shown to produce insulin resistance. In another recent study, prenatally androgenized females exhibited impaired glucose tolerance without any increase in BW or fat, or change in insulin sensitivity. In these mice, glucose intolerance was associated with defective pancreatic islet function, leading to impaired glucose sensing and regulation of insulin secretion (17). Hence, future studies are required to elucidate if and how androgen action regulates pancreatic islet and insulin function. Body composition, insulin resistance, and plasma triglyceride and cholesterol levels were not influenced by long-term letrozole treatment, contrasting with reported rat PCOS models in which letrozole treatment increased BW, body fat, lean body mass, fat depot weights, and triglyceride and cholesterol levels (14, 26, 60). Additionally, long-term DHEA treatment in the current study had no effect on body fat, insulin resistance, or serum cholesterol or triglyceride levels, although it did reduce body and lean mass weight. This contrasts with short-term (20 day) DHEA treatment in other rodent PCOS models that did not alter BW (21, 61), but induced insulin resistance (21). These discrepancies identify limitations about the suitability of DHEA and letrozole treatment models to investigate metabolic mechanisms in the pathogenesis of PCOS.

For the first time in a mouse PCOS model, we reveal that the presence of hepatic steatosis is significantly increased by prenatal DHT administration in mice and by the long-term presence of DHT and DHEA. Women with PCOS are more likely to exhibit hepatic steatosis (nonalcoholic fatty liver disease), which is associated with insulin resistance and metabolic syndrome (62). In a recent sheep PCOS model, prenatal T exposure induced fat accumulation in the liver, an early sign of liver damage (63). Our findings extend the data from the prenatal androgenized sheep model to this more versatile and complementary mouse model, which, in concert, suggest that circulating androgen levels may play a role in hepatic dysfunction in women with PCOS.

The Rotterdam consensus criteria and the Androgen Excess-PCOS Societies recommend that the presence of 2 of the following 3 diagnostic criteria fulfills a diagnosis of PCOS: oligo-ovulation or anovulation, hyperandrogenism, and polycystic ovaries (2, 64, 65). Using these criteria, in the current study we have identified that long-term DHT treatment of female mice is the most congruent with clinical features of human PCOS (Table 2 summarizes features of the androgenized mouse models relative to PCOS). Along with these criteria, long-term DHT females also displayed antral follicle arrest, thickening of the

theca layer in antral follicles, and several metabolic PCOS features including obesity, increased body fat, adipocyte hypertrophy, and dyslipidemia. The presence of hemorrhagic cysts in letrozole mice, atypical for PCOS, and lack of PCOS features in the prenatal DHT and long-term DHEA mice raise doubt about the suitability of these models to investigate the etiology of PCOS. In summary, we have revealed that the more androgen-selective long-term DHT treatment in female mice replicates a breadth of PCOS features and thus provides the most informative whole-animal approach in mice.

Acknowledgments

We thank Jenny Spaliviero and Lucy Yang for technical support, Bone Biology Laboratory, in particular Dr Tara Brennan-Speranza, at the ANZAC for assistance with the Lunar PIXImus Densitometer and insulin tolerance tests, Dr Maaike Kockx for assistance with triglyceride and cholesterol analysis, and Alessandra Warren for assistance with liver histologic analysis.

Address all correspondence and requests for reprints to: Dr Kirsty Walters, Andrology Laboratory, ANZAC Research Institute, Sydney, New South Wales 2139, Australia. E-mail: kwalters@anzac.edu.au.

This work was supported by Australian National Health and Medical Research Council project grant (APP1022648) and Australian Research Council Discovery Early Career Research Award (DE120100796).

Disclosure Summary: The authors have nothing to disclose.

References

1. **Fauser BC, Tarlatzis BC, Rebar RW, et al.** Consensus on women's health aspects of polycystic ovary syndrome (PCOS): the Amsterdam ESHRE/ASRM-Sponsored 3rd PCOS Consensus Workshop Group. *Fertil Steril*. 2012;97:28–38.e25.
2. **Azziz R, Carmina E, Dewailly D, et al.** The Androgen Excess and PCOS Society criteria for the polycystic ovary syndrome: the complete task force report. *Fertil Steril*. 2009;91:456–488.
3. **Abbott DH, Barnett DK, Bruns CM, Dumesic DA.** Androgen excess fetal programming of female reproduction: a developmental aetiology for polycystic ovary syndrome? *Hum Reprod Update*. 2005;11:357–374.
4. **Goodarzi MO, Dumesic DA, Chazenbalk G, Azziz R.** Polycystic ovary syndrome: etiology, pathogenesis and diagnosis. *Nat Rev Endocrinol*. 2011;7:219–231.
5. **Padmanabhan V, Veiga-Lopez A.** Sheep models of polycystic ovary syndrome phenotype. *Mol Cell Endocrinol*. 2013;373:8–20.
6. **Walters KA, Allan CM, Handelsman DJ.** Rodent models for human polycystic ovary syndrome. *Biol Reprod*. 2012;86:149, 1–149.
7. **Franks S.** Animal models and the developmental origins of polycystic ovary syndrome: increasing evidence for the role of androgens in programming reproductive and metabolic dysfunction. *Endocrinology*. 2012;153:2536–2538.
8. **Manikkam M, Steckler TL, Welch KB, Inskeep EK, Padmanabhan V.** Fetal programming: prenatal testosterone treatment leads to follicular persistence/luteal defects; partial restoration of ovarian function by cyclic progesterone treatment. *Endocrinology*. 2006;147:1997–2007.
9. **Smith P, Steckler TL, Veiga-Lopez A, Padmanabhan V.** Developmental programming: differential effects of prenatal testosterone and dihydrotestosterone on follicular recruitment, depletion of follicular reserve, and ovarian morphology in sheep. *Biol Reprod*. 2009;80:726–736.
10. **Padmanabhan V, Veiga-Lopez A, Abbott DH, Recabarren SE, Herkimer C.** Developmental programming: impact of prenatal testosterone excess and postnatal weight gain on insulin sensitivity index and transfer of traits to offspring of overweight females. *Endocrinology*. 2010;151:595–605.
11. **Abbott DH, Nicol LE, Levine JE, Xu N, Goodarzi MO, Dumesic DA.** Nonhuman primate models of polycystic ovary syndrome. *Mol Cell Endocrinol*. 2013;373:21–28.
12. **Dumesic DA, Abbott DH, Eisner JR, Goy RW.** Prenatal exposure of female rhesus monkeys to testosterone propionate increases serum luteinizing hormone levels in adulthood. *Fertil Steril*. 1997;67:155–163.
13. **van Houten EL, Kramer P, McLuskey A, Karels B, Themmen AP, Visser JA.** Reproductive and metabolic phenotype of a mouse model of PCOS. *Endocrinology*. 2012;153:2861–2869.
14. **Manneråas L, Cajander S, Holmäng A, et al.** A new rat model exhibiting both ovarian and metabolic characteristics of polycystic ovary syndrome. *Endocrinology*. 2007;148:3781–3791.
15. **Tyndall V, Broyde M, Sharpe R, Welsh M, Drake AJ, McNeilly AS.** Effect of androgen treatment during foetal and/or neonatal life on ovarian function in prepubertal and adult rats. *Reproduction*. 2012;143:21–33.
16. **Wu XY, Li ZL, Wu CY, et al.** Endocrine traits of polycystic ovary syndrome in prenatally androgenized female Sprague-Dawley rats. *Endocr J*. 2010;57:201–209.
17. **Roland AV, Nunemaker CS, Keller SR, Moenter SM.** Prenatal androgen exposure programs metabolic dysfunction in female mice. *J Endocrinol*. 2010;207:213–223.
18. **Beloosesky R, Gold R, Almog B, et al.** Induction of polycystic ovary by testosterone in immature female rats: modulation of apoptosis and attenuation of glucose/insulin ratio. *Int J Mol Med*. 2004;14:207–215.
19. **Edwards DA.** Neonatal administration of androstenedione, testosterone or testosterone propionate: effects on ovulation, sexual receptivity and aggressive behavior in female mice. *Physiol Behav*. 1971;6:223–228.
20. **Sullivan SD, Moenter SM.** Prenatal androgens alter GABAergic drive to gonadotropin-releasing hormone neurons: implications for a common fertility disorder. *Proc Natl Acad Sci USA*. 2004;101:7129–7134.
21. **Sander V, Luchetti CG, Solano ME, et al.** Role of the N, N′-dimethylbiguanide metformin in the treatment of female prepuberal BALB/c mice hyperandrogenized with dehydroepiandrosterone. *Reproduction*. 2006;131:591–602.
22. **Familiari G, Toscano V, Motta PM.** Morphological studies of polycystic mouse ovaries induced by dehydroepiandrosterone. *Cell Tissue Res*. 1985;240:519–528.
23. **Ward RC, Costoff A, Mahesh VB.** The induction of polycystic ovaries in mature cycling rats by the administration of dehydroepiandrosterone (DHA). *Biol Reprod*. 1978;18:614–623.
24. **Lee MT, Anderson E, Lee GY.** Changes in ovarian morphology and serum hormones in the rat after treatment with dehydroepiandrosterone. *Anat Rec*. 1991;231:185–192.
25. **Kafali H, Iriadam M, Ozardali I, Demir N.** Letrozole-induced polycystic ovaries in the rat: a new model for cystic ovarian disease. *Arch Med Res*. 2004;35:103–108.
26. **Sasikala SL, Shamila S.** Unique rat model exhibiting biochemical fluctuations of letrozole induced polycystic ovary syndrome and

subsequent treatment with allopathic and ayurvedic medicines. *J Cell Tissue Res*. 2009;9:2013–2017.
27. **Linder CC.** Genetic variables that influence phenotype. *ILAR J*. 2006;47:132–140.
28. **Walters KA, Allan CM, Jimenez M, et al.** Female mice haploinsufficient for an inactivated androgen receptor (AR) exhibit age-dependent defects that resemble the AR null phenotype of dysfunctional late follicle development, ovulation, and fertility. *Endocrinology*. 2007;148:3674–3684.
29. **Simanainen U, Gao YR, Walters KA, et al.** Androgen resistance in female mice increases susceptibility to DMBA-induced mammary tumors. *Horm Cancer*. 2012;3:113–124.
30. **Singh J, O'Neill C, Handelsman DJ.** Induction of spermatogenesis by androgens in gonadotropin-deficient (hpg) mice. *Endocrinology*. 1995;136:5311–5321.
31. **Stener-Victorin E, Holm G, Labrie F, Nilsson L, Janson PO, Ohlsson C.** Are there any sensitive and specific sex steroid markers for polycystic ovary syndrome? *J Clin Endocrinol Metab*. 2010;95:810–819.
32. **Walters KA, Middleton LJ, Joseph SR, et al.** Targeted loss of androgen receptor signaling in murine granulosa cells of preantral and antral follicles causes female subfertility. *Biol Reprod*. 2012;87:151.
33. **Myers M, Britt KL, Wreford NG, Ebling FJ, Kerr JB.** Methods for quantifying follicular numbers within the mouse ovary. *Reproduction*. 2004;127:569–580.
34. **van Casteren JI, Schoonen WG, Kloosterboer HJ.** Development of time-resolved immunofluorometric assays for rat follicle-stimulating hormone and luteinizing hormone and application on sera of cycling rats. *Biol Reprod*. 2000;62:886–894.
35. **Jimenez M, Spaliviero JA, Grootenhuis AJ, Verhagen J, Allan CM, Handelsman DJ.** Validation of an ultrasensitive and specific immunofluorometric assay for mouse follicle-stimulating hormone. *Biol Reprod*. 2005;72:78–85.
36. **Harwood DT, Handelsman DJ.** Development and validation of a sensitive liquid chromatography-tandem mass spectrometry assay to simultaneously measure androgens and estrogens in serum without derivatization. *Clin Chim Acta*. 2009;409:78–84.
37. **McNamara KM, Harwood DT, Simanainen U, Walters KA, Jimenez M, Handelsman DJ.** Measurement of sex steroids in murine blood and reproductive tissues by liquid chromatography-tandem mass spectrometry. *J Steroid Biochem Mol Biol*. 2010;121:611–618.
38. **Brennan-Speranza TC, Henneicke H, Gasparini SJ, et al.** Osteoblasts mediate the adverse effects of glucocorticoids on fuel metabolism. *J Clin Invest*. 2012;122:4172–4189.
39. **Kleiner DE, Brunt EM, Van Natta M, et al.** Design and validation of a histological scoring system for nonalcoholic fatty liver disease. *Hepatology*. 2005;41:1313–1321.
40. **Franks S, McCarthy MI, Hardy K.** Development of polycystic ovary syndrome: involvement of genetic and environmental factors. *Int J Androl*. 2006;29:278–285; discussion 286–290.
41. **Dowling AR, Nedorezov LB, Qiu X, Marino JS, Hill JW.** Genetic factors modulate the impact of pubertal androgen excess on insulin sensitivity and fertility. *PLoS One*. 2013;8:e79849.
42. **Abbott DH, Padmanabhan V, Dumesic DA.** Contributions of androgen and estrogen to fetal programming of ovarian dysfunction. *Reprod Biol Endocrinol*. 2006;4:17.
43. **Franks S, Stark J, Hardy K.** Follicle dynamics and anovulation in polycystic ovary syndrome. *Hum Reprod Update*. 2008;14:367–378.
44. **Vendola KA, Zhou J, Adesanya OO, Weil SJ, Bondy CA.** Androgens stimulate early stages of follicular growth in the primate ovary. *J Clin Invest*. 1998;101:2622–2629.
45. **Wang H, Andoh K, Hagiwara H, et al.** Effect of adrenal and ovarian androgens on type 4 follicles unresponsive to FSH in immature mice. *Endocrinology*. 2001;142:4930–4936.
46. **Murray AA, Gosden RG, Allison V, Spears N.** Effect of androgens on the development of mouse follicles growing in vitro. *J Reprod Fertil*. 1998;113:27–33.
47. **Forsdike RA, Hardy K, Bull L, et al.** Disordered follicle development in ovaries of prenatally androgenized ewes. *J Endocrinol*. 2007;192:421–428.
48. **West C, Foster DL, Evans NP, Robinson J, Padmanabhan V.** Intrafollicular activin availability is altered in prenatally-androgenized lambs. *Mol Cell Endocrinol*. 2001;185:51–59.
49. **Abbott DH, Dumesic DA, Eisner JR, Colman RJ, Kemnitz JW.** Insights into the development of polycystic ovary syndrome (PCOS) from studies in prenatally androgenized female rhesus monkeys. *Trends Endocrinol Metab*. 1998;9:62–67.
50. **Britt KL, Drummond AE, Cox VA, et al.** An age-related ovarian phenotype in mice with targeted disruption of the Cyp 19 (aromatase) gene. *Endocrinology*. 2000;141:2614–2623.
51. **Schomberg DW, Couse JF, Mukherjee A, et al.** Targeted disruption of the estrogen receptor-alpha gene in female mice: characterization of ovarian responses and phenotype in the adult. *Endocrinology*. 1999;140:2733–2744.
52. **Kumar TR, Palapattu G, Wang P, et al.** Transgenic models to study gonadotropin function: the role of follicle-stimulating hormone in gonadal growth and tumorigenesis. *Mol Endocrinol*. 1999;13:851–865.
53. **Luchetti CG, Solano ME, Sander V, et al.** Effects of dehydroepiandrosterone on ovarian cystogenesis and immune function. *J Reprod Immunol*. 2004;64:59–74.
54. **Mahesh VB, Greenblatt RB.** Isolation of dehydroepiandrosterone and 17alpha-hydroxy-delta5-pregenolone from the polycystic ovaries of the Stein-Leventhal syndrome. *J Clin Endocrinol Metab*. 1962;22:441–448.
55. **Matsuzawa Y.** The metabolic syndrome and adipocytokines. *FEBS Lett*. 2006;580:2917–2921.
56. **Barber TM, Franks S.** Adipocyte biology in polycystic ovary syndrome. *Mol Cell Endocrinol*. 2013;373:68–76.
57. **Chen X, Jia X, Qiao J, Guan Y, Kang J.** Adipokines in reproductive function: a link between obesity and polycystic ovary syndrome. *J Mol Endocrinol*. 2013;50:R21–R37.
58. **Wild RA.** Dyslipidemia in PCOS. *Steroids*. 2012;77:295–299.
59. **Lee YH, Pratley RE.** The evolving role of inflammation in obesity and the metabolic syndrome. *Curr Diab Rep*. 2005;5:70–75.
60. **Maliqueo M, Sun M, Johansson J, et al.** Continuous administration of a P450 aromatase inhibitor induces polycystic ovary syndrome with a metabolic and endocrine phenotype in female rats at adult age. *Endocrinology*. 2013;154:434–445.
61. **Roy S, Mahesh VB, Greenblatt RB.** Effect of dehydroepiandrosterone and delta4-androstenedione on the reproductive organs of female rats: production of cystic changes in the ovary. *Nature*. 1962;196:42–43.
62. **Karoli R, Fatima J, Chandra A, Gupta U, Islam FU, Singh G.** Prevalence of hepatic steatosis in women with polycystic ovary syndrome. *J Hum Reprod Sci*. 2013;6:9–14.
63. **Hogg K, Wood C, McNeilly AS, Duncan WC.** The in utero programming effect of increased maternal androgens and a direct fetal intervention on liver and metabolic function in adult sheep. *PLoS One*. 2011;6:e24877.
64. **Rotterdam ESHRE/ASRM-sponsored PCOS consensus workshop group.** Revised 2003 consensus on diagnostic criteria and long-term health risks related to polycystic ovary syndrome (PCOS). *Hum Reprod* 2004;19:41–47.
65. **Azziz R, Carmina E, Dewailly D, et al.** Positions statement: criteria for defining polycystic ovary syndrome as a predominantly hyperandrogenic syndrome: an Androgen Excess Society guideline. *J Clin Endocrinol Metab*. 2006;91:4237–4245.